

Climatology of ionospheric *F*-region disturbances

Dimitris N. Fotiadis ⁽¹⁾, Stamatis S. Kouris ⁽¹⁾, Vincenzo Romano ⁽²⁾ and Bruno Zolesi ⁽²⁾

⁽¹⁾ *Electrical and Computer Engineering Department, Aristotle University of Thessaloniki, Greece*

⁽²⁾ *Istituto Nazionale di Geofisica e Vulcanologia, Roma, Italy*

Abstract

After more than 60 years of research, ionospheric disturbances are today a most challenging topic of upper atmospheric physics. Although the understanding of the thermosphere-ionosphere system has increased, quantitative predictions of ionospheric perturbations, valid for space weather assessment, are still imprecise. Using a long f_oF2 dataset, an analytical climatology of the *F*-region storms is presented as a function of appropriate variables. Local phenomena are then detected.

Key words *ionosphere – F2-layer critical frequency – ionospheric disturbances*

1. Introduction

Ionospheric disturbances, being manifestations of extreme space weather, may severely degrade terrestrial and earth-to-satellite technological systems. Consequently, long-term predictions and short-term forecasting of such phenomena are essential. Recent investigations, mainly by global-scale numerical simulations of first-principle models (Schunk, 1996) and by measurement studies (Yeh *et al.*, 1994), have improved our understanding of the thermosphere-ionosphere system. However, the agreement between simulations and observations is still rather qualitative, whereas a quantitative modeling for immediate space weather application has not been achieved yet (Szuszczewicz *et al.*, 1998; Fuller-Rowell *et al.*, 2000).

One way to establish accurate specification of the temporal and spatial development of a ionospheric storm is to fully understand disturbance mechanisms and insert suitable input to the global simulation models. Although research has grown rapidly in this direction (Prölss, 1993, 1995; Buonsanto, 1999; Mikhailov, 2000), cause-effect relationships are hard to establish in many cases. Alternatively, ionospheric empirical storm-time models in disturbed magnetic conditions have been developed (*e.g.*, Cander and Mihajlovic, 1998), improving thus existing ionospheric empirical models (Araujo-Pradere *et al.*, 2002, 2003). Such an advance deals with one major cause of ionospheric storms, hence not with the only one, since ionospheric storms can be regional and are not directly linked to geomagnetic activity (Wilkinson, 1995).

Another potential way of storm modeling is first to produce a detailed climatology and morphology of ionospheric storm independently of the cause-effect mechanisms and then correlate those morphologies presenting important frequency of occurrence in time and space, with certain physical parameters so as to improve long-term predictions. It is in this latter direction that this work contributes, providing radio users and researchers with an analytical climatology

Mailing address: Dr. Dimitris N. Fotiadis, National Telecommunications and Post Commission (EETT), 60 Kifisias Ave., 15125 Marousi, Greece; e-mail: dfot@eett.gr

which is expressed with caution to appropriate variables and prominent features of ionospheric storms, also emphasizing regional phenomena.

2. Definitions and method of analysis

Distinct from any geophysical definition of storminess, Kouris *et al.* (1998, 1999) have developed a *ionospheric* definition of disturbed days and periods for the day-to-day variability of the $F2$ -layer critical frequency (df_oF2). This definition of disturbances is based solely on their power, amplitude and duration, being consistent with suggestions of other workers (Gulyaeva, 1996).

Initially, day-to-day variability of f_oF2 was calculated with the transformation: $df_oF2=(f_oF2+$

$-f_oF2_{\text{median}})/f_oF2_{\text{median}}$, for each hour, day, month, year, station of table I. Then, the algorithm for disturbed periods (Kouris *et al.*, 1999) was applied. Thus, a catalogue of positive and negative F -region disturbances was compiled.

In order to sufficiently illustrate ionospheric disturbances' climatology in time and space and to avoid grouping storms of different mechanisms and morphological aspects, the climatology of disturbances is presented according to:

i) Their *phase*, positive or negative, since it is attributed to different disturbance mechanisms (*e.g.*, Prölss, 1995).

ii) Their *season*, since it is long supported that seasonal variations are prominent features of ionospheric storms and directly linked to their phase. In this work each month has been dealt with separately.

Table I. List of stations and years of f_oF2 data used in the analysis. The geomagnetic latitude is calculated by the International Geomagnetic Reference Field for the year 1986 for a 300 km height. Dip inclination angle and Modip (Rawer, 1963) are calculated for 1980.

Station	Station Code	Geographic		IGRF Corrected			Years of data
		Lat. (°)	Long. (°)	Geomagnetic Lat. (°)	Dip (°)	Modip (°)	
Nicosia	NIC	35.1	33.2	28.5	50.8	44.4	87-96
El Arenosillo	ARE	37.1	353.2	30.5	52.2	45.6	82, 83, 93-96
Gibilmana	GIB	37.6	14	30.4	52.8	46.0	76-94
Tortosa	TOR	40.8	0.5	34.8	56.4	48.5	64-87, 91-95
Rome	ROM	41.8	12.5	35.7	57.6	49.4	76-94, 96
Grocka	GRO	44.8	20.5	39.4	61.1	51.7	85-93
Poitiers	POI	46.6	0.3	42.3	62.3	52.7	64-94
Freiburg	FRE	48.1	7.6	43.6	63.7	53.7	64-74
Lannion	LAN	48.8	356.6	45.4	64.3	54.1	64-94
Kiev	KIE	50.5	30.5	45.8	66.5	55.5	64-92
Slough	SLO	51.5	359.4	48.4	66.5	55.8	67-95
Juliusruh	JUL	54.6	13.4	50.8	68.9	57.7	64-95
Moscow	MOS	55.5	37.3	51	70.4	58.5	64-96
Uppsala	UPP	59.8	17.6	56.3	72.4	60.7	64-96
Leningrad	LEN	60	30.7	55.9	72.9	60.9	64-96
Arkhangelsk	ARK	64.4	40.5	60	75.8	63.6	69-93
Lycksele	LYC	64.7	18.8	61.3	75.2	63.5	64-96
Sodankyla	SOD	67.4	26.6	63.6	76.8	65.2	64-89
Kiruna	KIR	67.8	20.4	64.4	76.8	65.4	64-86, 91-96
Loparskaya	LOP	68	33	63.9	77.3	65.6	64-77, 81-84, 91-96
Dakar	DAK	14.8	341.6	2.9	16.1	16.0	64-89
Johannesburg	JOH	-26.1	28.1	-35.6	-62.0	-48.8	64, 67-91
Grahamstown	GRW	-33.3	26.5	-41.2	-64.2	-50.8	74-76, 78-84, 86-96
Syowa Base	SYO	-69	39.6	-66.4	-66.7	-62.8	66, 68-79

Table I (*continued*).

Singapore	SIN	1.3	103.8	-7.7	-17.6	-17.1	64-71
Kodaikanal	KOD	10.2	77.5	1.6	3.7	3.8	64-80, 85, 86
Manila	MAN	14.6	121.1	6.2	14.2	14.1	64-94
Taipei	TAI	25	121.5	17.5	34.9	32.6	64-96
Okinawa	OKI	26.3	127.8	18.8	36.6	34.0	64-88
Yamagawa	YAM	31.2	130.6	23.8	43.9	39.7	64-88
Kokubunji	KOK	35.7	139.5	28.2	48.8	43.4	64-90
Ashkhabad	ASH	37.9	58.3	32.6	55.8	47.6	64-86, 89-95
Akita	AKI	39.7	140.1	32.3	53.5	46.8	64-89
Wakkanai	WAK	45.4	141.7	38.1	59.4	51.1	64-88
Karaganda	KAR	49.8	73.1	44.8	68.1	56.0	64-88
Irkutsk	IRK	52.5	104	46.8	71.0	57.8	64-90
Tomsk	TOM	56.5	84.9	51.4	74.1	60.1	64-90, 92-96
Magadan	MAG	60	151	53.2	71.2	60.4	68-96
Yakutsk	YAK	62	129.6	55.5	75.6	62.6	64-91
Provideniya Bay	PRO	64.4	186.6	60.3	73.9	63.0	64-70, 79-83
Norilsk	NRI	69.4	88.1	63.8	82.0	67.5	68-88
Tiksibay	TIK	71.6	128.9	65.2	82.0	68.6	64-71, 87
Dikson	DIK	73.5	80.4	67.7	83.3	69.9	82-96
Vanimo	VAN	-2.7	141.3	-11.4	-22.5	-21.5	64, 65, 67-93
Darwin	DAR	-12.4	130.9	-22.2	-40.8	-35.8	83-88, 90-94
Townsville	TOW	-19.3	146.7	-28.7	-49.1	-41.4	64-95
Brisbane	BRI	-27.5	152.9	-36.8	-58.1	-47.1	64-86
Norfolk	NOR	-29	168	-35.9	-56.8	-46.7	64-94
Mundaring	MUN	-32	116.2	-44.5	-66.7	-51.7	64-94
Canberra	CAN	-35.3	149	-45.8	-66.4	-52.1	64-91, 93, 94
Christchurch	CHR	-43.6	172.8	-50.3	-69.0	-54.8	64-70
Kerguelen	KER	-49.4	70.3	-58.4	-68.6	-56.0	65-84, 87, 88
Campbell Island	CLL	-52.5	169.2	-60.2	-76.0	-59.5	70-85
Macquarie Island	MAC	-54.5	159	-64.4	-79.2	-61.1	84-92
Casey	CAS	-66.3	110.5	-80.7	-82.3	-66.2	64-74, 90, 91
Mawson	MAW	-67.6	62.9	-70.5	-70.1	-63.2	64-87, 91-93
Davis	DAV	-68.6	77.9	-74.8	-73.6	-64.8	85-88, 90, 91, 93
Scott Base	SCO	-77.9	166.8	-79.9	-82.0	-72.3	70-83
Maui	MAU	20.8	203.5	21.3	38.5	34.8	64-94
Point Arguello	PNT	34.6	239.4	40.5	59.8	49.0	72-74, 77-96
Wallops Island	WAL	37.8	284.5	49.5	68.0	53.2	67-87, 91-96
Boulder	BOU	40	254.7	49.1	67.6	53.4	64-96
Ottawa	OTT	45.4	284.1	56.9	73.6	56.9	64-93
St. Johns	STJ	47.6	307.3	55.2	70.3	56.2	66-77
Winnipeg	WIN	49.8	265.6	60.7	76.8	59.1	66-76
Goosebay	GOO	53.3	299.2	62.6	75.8	59.7	87-96
Churchill	CHU	58.8	265.8	69.5	82.5	63.4	66-74
College	COL	64.9	212.2	65	77.1	64.2	64-67, 88, 89, 91, 94
Resolute Bay	RES	74.7	265.1	83.8	89.0	71.7	64-91
Huancayo	HUA	-12	284.7	1.4	1.9	1.9	64-87
Tahiti	TAH	-17.7	210.7	-16.3	-30.8	-28.9	71-89
Concepcion	CON	-36.6	287	-22.5	-36.4	-35.3	64-79
Port Stanley	POR	-51.7	302.2	-37.3	-49.2	-47.5	64-92
Argentine Is.	ARI	-65.2	295.7	-49.8	-59.2	-57.9	64-92
Halley Bay	HAL	-75.5	333.4	-61.5	-65.4	-66.3	64-80

iii) Their *local time* (LT) of commencement (Jones, 1971; Prölss and von Zahn, 1978; Danilov and Morozova, 1985; Prölss, 1993). A disturbance may commence any time during the day; on the other hand, a minimum frequency of occurrence of such phenomena should be ensured, without harming the analytical picture. Thus, by calculating the solar zenith angle at 300 km height, we have defined four local-time zones: day ($\cos\chi > 0.20$), night ($\cos\chi = 0$), while dawn and dusk fall in between.

iv) Their *universal time* (UT) of commencement by studying each station separately within its longitude sector and hemisphere (Fuller-Rowell, 1994; Hajkowicz, 1998). Furthermore, investigating climatology in this way may reveal *regional (local)* phenomena (Cander, 1993).

v) Their *duration*. This morphological aspect – rather than the depth – is directly linked to different disturbance mechanisms, especially on positive storm effects (Buonsanto, 1999). Therefore, before stepping to climatology, the basic morphological features, depth and duration, need to be investigated.

3. Results and discussion

3.1. Basic morphology

Table II shows the percentage of positive and negative storms for which the respective variability level (*i.e.* the deviation from the monthly median) is not exceeded, giving thus the cumulative depth distribution for 54 ionospheric stations in different longitudes and latitudes. Selecting as a boundary 49% of the total number of disturbances, positive disturbances display an important variation of depth with the geomagnetic latitude in different longitude sectors. A stable distribution is observed in mid-latitudes up to about $55^\circ\varphi_m$. In higher latitudes positive storms become deeper, being more intense around $62^\circ\varphi_m$, boundary of auroral oval. Then, phenomena seem to be less deep at about $70^\circ\varphi_m$, however they are somewhat deeper in the polar region. Furthermore, positive storms always grow deeper approaching the geomagnetic equator.

On the contrary, negative storm effects are more shallow and their depth distribution may not

Table II. Percentage of positive (*left*) and negative (*right*) disturbances which does not exceed the respective variability level – ‘depth’ (*x*-axis). Greek ‘ Σ ’ denotes total percentage of positive/negative storms. Top to bottom: European, Asian, Australian and North American stations.

φ_m	.4	.5	.6	.7	.8	.9	1	Σ	–.4	–.45	–.5	–.6	–.7	–.8	–.9	–1	Σ
64.4 KIR	14	31	40	45	49	52	54	57	16	26	33	41	43				
63.9 LOP	14	32	43	49	52	54	55	56	15	26	33	42	42	43	44		
63.6 SOD	10	24	35	42	46	49	50	54	13	24	33	43	46				
61.3 LYC	9	23	33	40	44	47	49	56	13	23	30	41	44				
60 ARK	11	25	35	41	45	47	49	56	15	26	33	42	44				
56.3 UPP	13	30	40	45	48	49	51	54	17	27	33	43	45	46			
55.9 LEN	13	30	41	45	48	50	51	54	17	27	33	42	45	46			
51 MOS	18	39	48	54	55	55	56		21	32	37	42	44				
50.8 JUL	18	38	48	52	53	54			21	31	37	44	46				
48.4 SLO	18	38	48	52	54	55			22	32	38	43	45				
45.8 KIE	20	38	49	52	54	54	54	55	24	35	40	44	45				
45.4 LAN	19	37	47	51	53	53	54		25	35	41	45	46				
42.3 POI	18	39	50	54	56	57			23	34	39	42	43				
35.7 ROM	22	46	57	61	63	63	63	64	21	30	33	36					

Table II (continued).

ϕ_m	.4	.5	.6	.7	.8	.9	1	Σ	-.4	-.45	-.5	-.6	-.7	-.8	-.9	-1	Σ
34.8 TOR	19	44	58	62	66	67			20	28	31	33					
30.4 GIB	17	39	53	61	65	66	66	67	16	25	30	33					
63.8 NRI	9	23	33	41	46	48	50	54	14	24	31	43	46				
55.5 YAK	13	32	42	48	50	52	52	54	18	28	35	43	46				
53.2 MAG	14	33	45	50	52	53	53	55	19	30	36	42	44	45			
51.4 TOM	19	40	50	56	58	58	58	59	22	32	35	40	40	41			
46.8 IRK	19	41	51	55	57	57	58		22	32	37	42					
32.3 AKI	21	43	58	64	66	67	67	70	18	25	28	30					
28.2 KOK	20	45	58	64	67	68	69	71	18	25	27	28	29				
23.8 YAM	17	44	59	67	71	74	75	79	12	18	20	21					
18.8 OKI	11	31	46	56	62	65	68	72	15	22	26	28					
17.5 TAI	9	26	40	50	56	60	62	66	15	25	30	34					
6.2 MAN	9	23	34	43	49	52	54	59	14	25	33	40	41				
-7.7 SIN	5	20	33	41	45	49	52	55	15	25	34	43	45				
-11.4 VAN	7	21	31	39	44	48	50	55	14	24	33	42	45				
-22.2 DAR	12	32	46	53	58	62	63	67	16	24	28	33					
-28.7 TOW	17	39	52	58	61	62	63	64	21	29	33	36					
-35.9 NOR	21	45	56	60	61	62			22	30	34	37	38				
-36.8 BRI	21	46	57	61	62	63	63	64	22	30	33	36					
-44.5 MUN	21	41	50	53	54	55			23	33	39	44	45				
-45.8 CAN	19	39	47	50	51				27	36	42	48	49				
-54.2 HOB	14	34	46	52	55	56	57	58	19	29	34	47	42				
-58.4 KER	11	27	37	44	48	52	54	61	16	24	30	31	39				
-60.2 CLL	11	25	35	41	44	46	47	50	18	29	37	46	50				
-64.4 MAC	11	29	40	44	47	49	51	53	20	32	38	46	47				
-70.5 MAW	12	33	46	54	59	61	62	64	15	24	30	35	36				
-74.8 DAV	6	23	39	57	55	59	60	66	13	22	28	33	34				
-79.9 SCO	8	23	35	43	47	51	53	57	11	21	28	39	42	43			
-80.7 CAS	8	24	36	46	52	54	56	62	13	23	30	37	38				
83.8 RES	6	21	33	41	47	50	52	57	14	24	32	41	43				
69.5 CHU	15	32	42	48	51	52	52	54	19	31	38	45	46				
65 COL	10	25	34	41	44	47	49	59	13	22	29	39	40	41			
62.6 GOO	9	22	32	39	43	45	46	52	12	21	29	41	46	48			
60.7 WIN	11	25	33	38	43	45	46	56	15	24	29	41	44				
56.9 OTT	15	33	41	44	46	47			19	30	39	49	52	53			
55.2 STJ	12	29	39	44	46	47	47	48	15	28	35	47	51	52			
49.5 WAL	17	35	45	48	50	51	51	52	22	32	38	46	48				
49.1 BOU	20	41	51	56	58	59	60		22	29	33	38	40				
40.5 PNT	18	39	52	59	63	65	66	69	16	22	26	30	31				
21.3 MAU	9	25	38	47	53	58	60	67	15	25	30	33					

be interpreted using the above method. Negative disturbances are deeper around $55^\circ \varphi_m$ and $65^\circ \varphi_m$, at the edge of auroral oval boundary which moves under geomagnetically disturbed conditions. On the other hand, negative storms are more shallow (about -50% of the monthly median f_oF2) in low midlatitudes ($22-35^\circ \varphi_m$) and the equatorial anomaly crest ($15-22^\circ \varphi_m$), but they are somewhat deeper on the geomagnetic equator.

Figure 1 shows cumulative distributions of the duration of positive/negative disturbances in Asian and Australian stations. Accordingly, we calculated the duration threshold for which the gradient of the distribution tends to zero, defining thus a maximum duration. We assess that the above criterion may be satisfied with a potential error of 1% between sequential distribution values. Figure 2 illustrates the respective thresholds for positive and negative disturbances with the geomagnetic latitude. Since much dispersion of

values is observed, we have drawn two polynomial regression lines.

It is evident from fig. 2 that the greatest duration of positive storms is not more than 15 h and it is observed in higher midlatitudes ($55-60^\circ \varphi_m$) and the upper boundary of the equatorial anomaly crest ($20-25^\circ \varphi_m$). In midlatitudes great dispersion of this maximum duration is observed which may be attributed to a longitudinal dependence (Fotiadis *et al.*, 2004) and the regional character of positive disturbances (Hajkowicz, 1998). From $60^\circ \varphi_m$ polewards maximum observed duration is delimited to 12 h and even more in the polar region (10 h), as also happens on the geomagnetic equator region. On the contrary, negative storm effects may last more than 15 h in midlatitudes ($55-60^\circ \varphi_m$). In higher and polar latitudes negative disturbances have a maximum duration of about 9-11 h while they appear to be shortest on the equator (7-8 h).

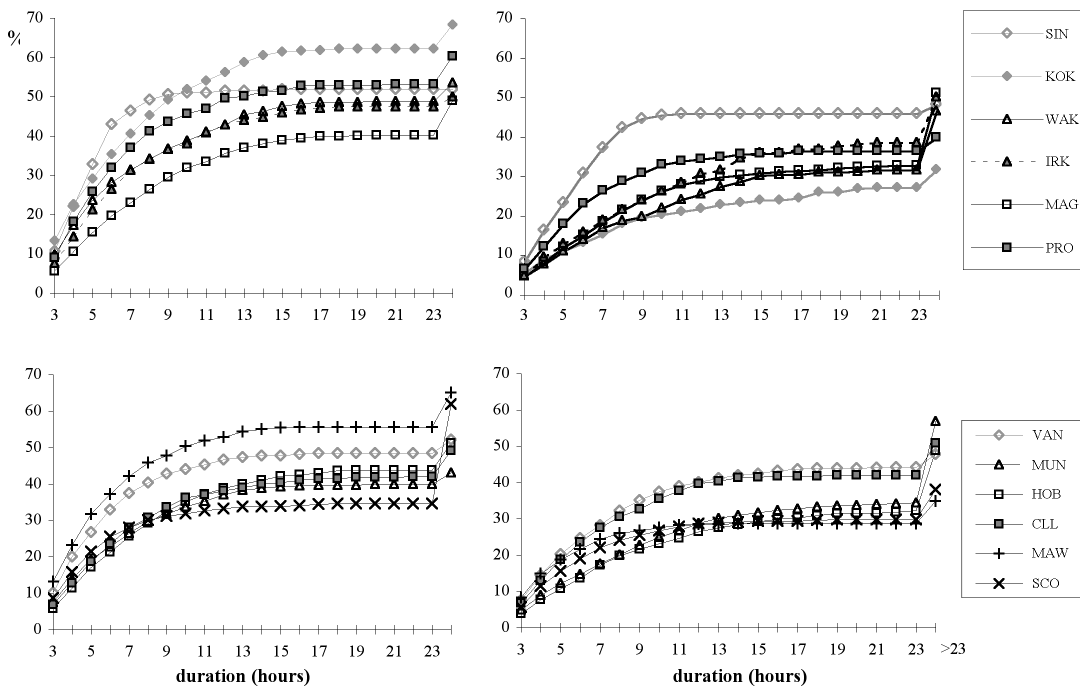


Fig. 1. Percentage of positive (*left*) and negative (*right*) disturbances for which the corresponding duration is not exceeded (cumulative distribution). *Top*: Asian stations; *bottom*: Australian stations.

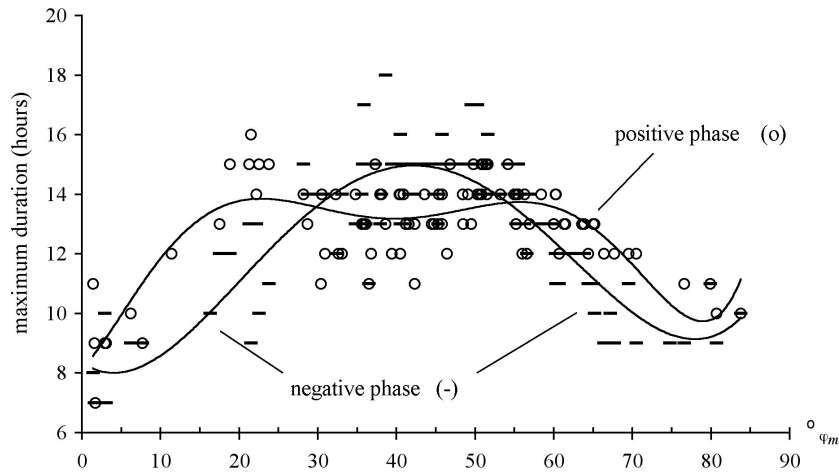


Fig. 2. Maximum duration of positive and negative disturbances with geomagnetic latitude.

Synoptically, it may be supported that where great depths are observed the duration of phenomena is delimited and *vice versa*. Definite exceptions are the equatorial anomaly crest and the higher-latitude boundary where the power of positive disturbances maximizes, since these regions constitute the 'source' of these phenomena.

3.2. Climatology of disturbances

In the previous section it is shown that phenomena last for about 16 h, however it should be stressed that a small amount of disturbances (mostly of negative phase) last for more than a day. In the literature, depending on their duration, disturbances are attributed to different mechanisms (*e.g.*, Hocke and Schlegel, 1996; Buonsanto, 1999). Similarly, three duration classes are selected here: i) 3-5 h, ii) 6-24 h and iii) more than 24 h.

The frequency of occurrence of positive and negative disturbances is presented in fig. 3a-d, and 4a-d respectively, according to the parameters mentioned in the method of analysis section. Comments on the results follow categorized by the local time of storm commencement:

Sunrise – Positive storms have mainly short duration and are observed with a frequency of

0.5-1 phenomena per month at 50-65° ϕ_m latitudes in Europe and Asia, whereas in Australia over 70° ϕ_m and only in equinox period. However, they occur more frequently in the American zone, at summer period over 60° ϕ_m and also sporadically at west coast mid- and low-latitude stations (Maui and Point Arguello). In winter such phenomena are limited only in short latitude strips well above 60° ϕ_m . Positive storms of greater duration mostly affect Europe than any other sector.

Negative disturbances of short duration are more infrequent than the positive ones, occurring mostly in near-summer months at 50-65° ϕ_m . Above 65° ϕ_m they are observed only in the American sector in equinox and winter months (polar region). Again, medium duration negative storms affect Europe in near-winter months. Negative storms commencing at sunrise are totally absent from low and lower mid-latitude stations.

Day – Positive storm effects appear to have short and medium duration and are a dominant feature of the equatorial anomaly crest (all year long) and lower midlatitude ionosphere (in summer). Such effects are also observed in greater midlatitudes hence at equinox, but never in winter. The above climatology is almost reversed

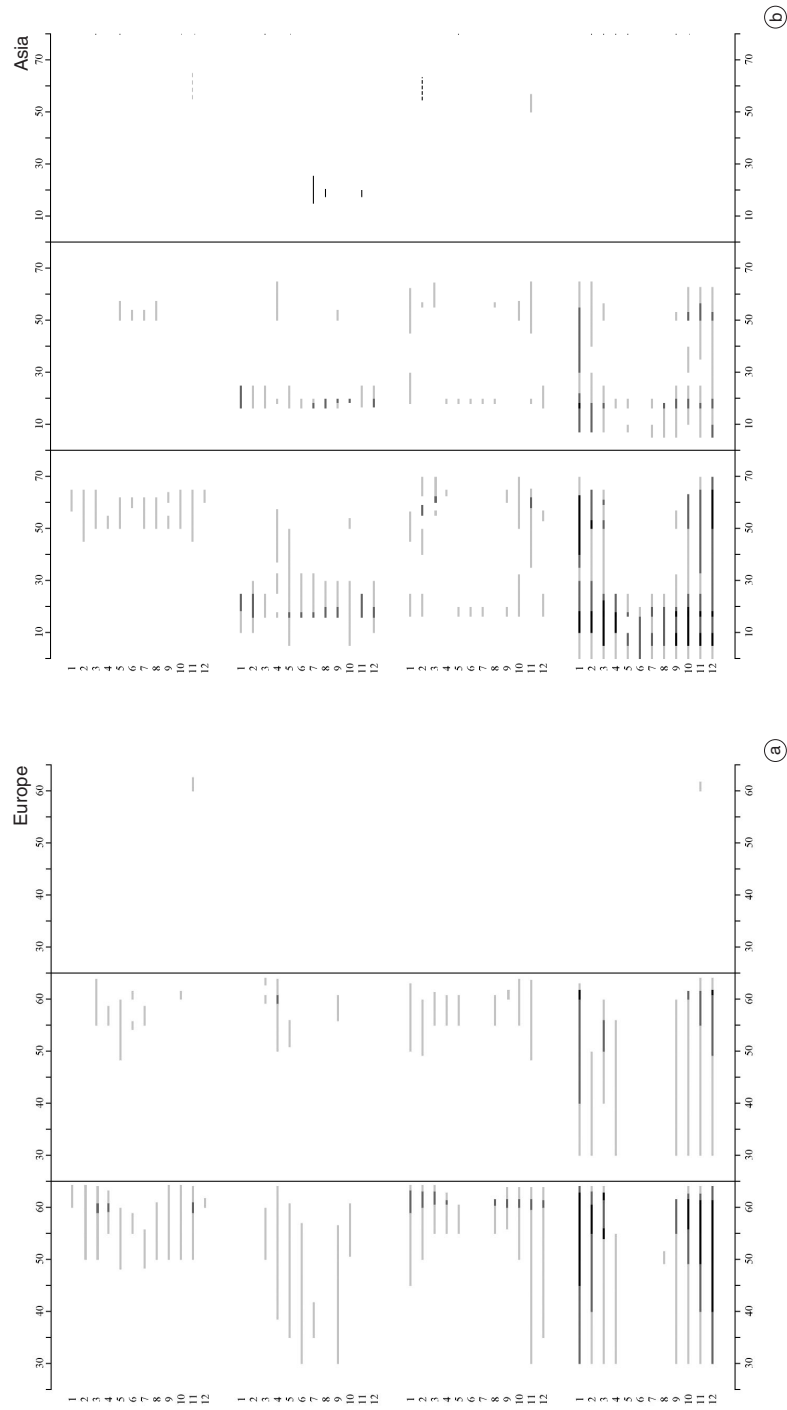


Fig. 3a,b. Frequency of occurrence of *positive* storms per month according to LT of commencement (from top to bottom: sunrise, day, sunset, night) and duration class (from left to right: small, medium, large duration) as a function of geomagnetic latitude (λ -axis) in (a) Europe and (b) Asia (light grey: 0.5-1 storms/month, grey: 1-2 storms/month, dark grey: 2-3 storms/month and black: > 3 storms/month).

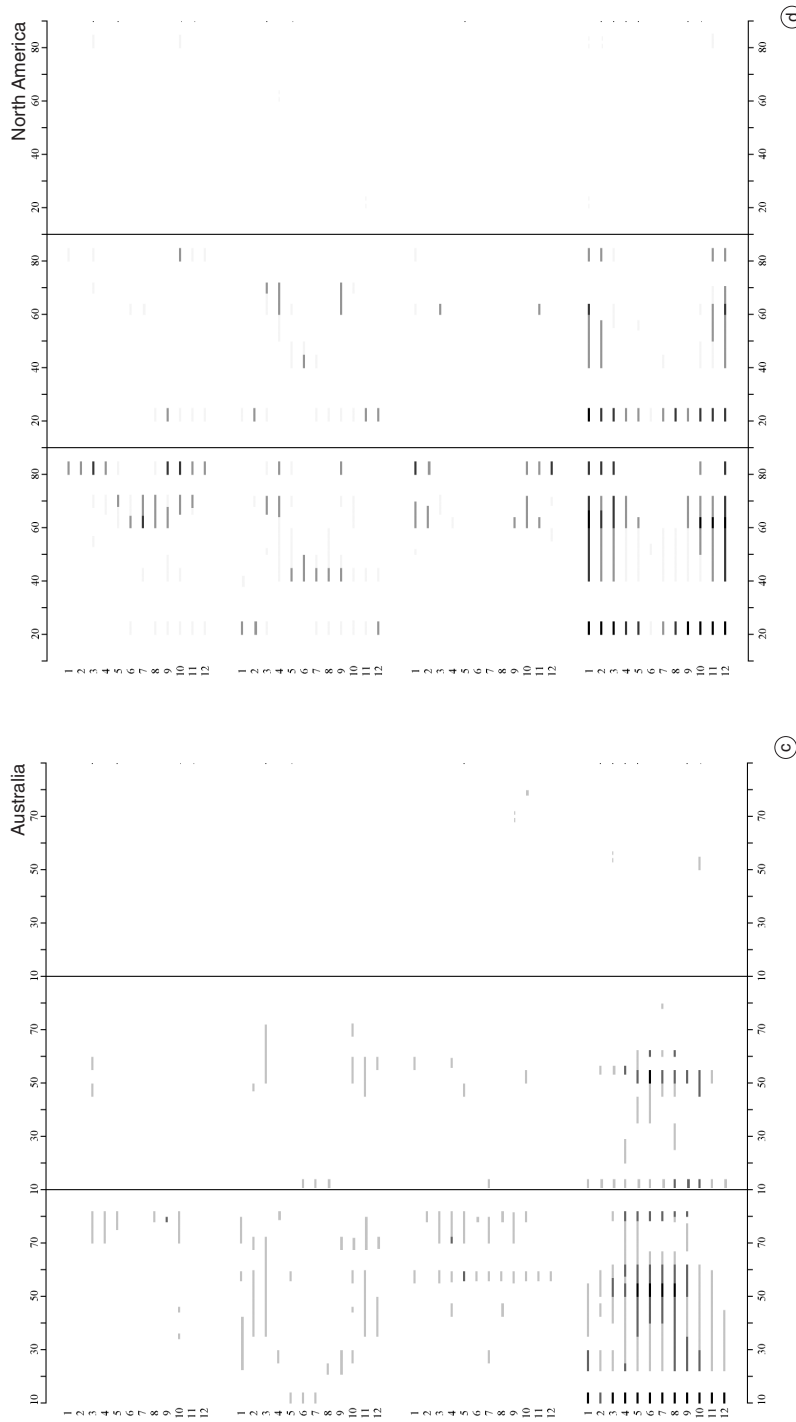


Fig. 3c,d. Frequency of occurrence of *positive* storms per month according to LT of commencement (from top to bottom: sunrise, day, sunset, night) and duration class (from left to right: small, medium, large duration) as a function of geomagnetic latitude (x-axis) in (c) Australia and (d) North America (light grey: 0.5-1 storms/month, dark grey: 1-2 storms/month, black: >3 storms/month).

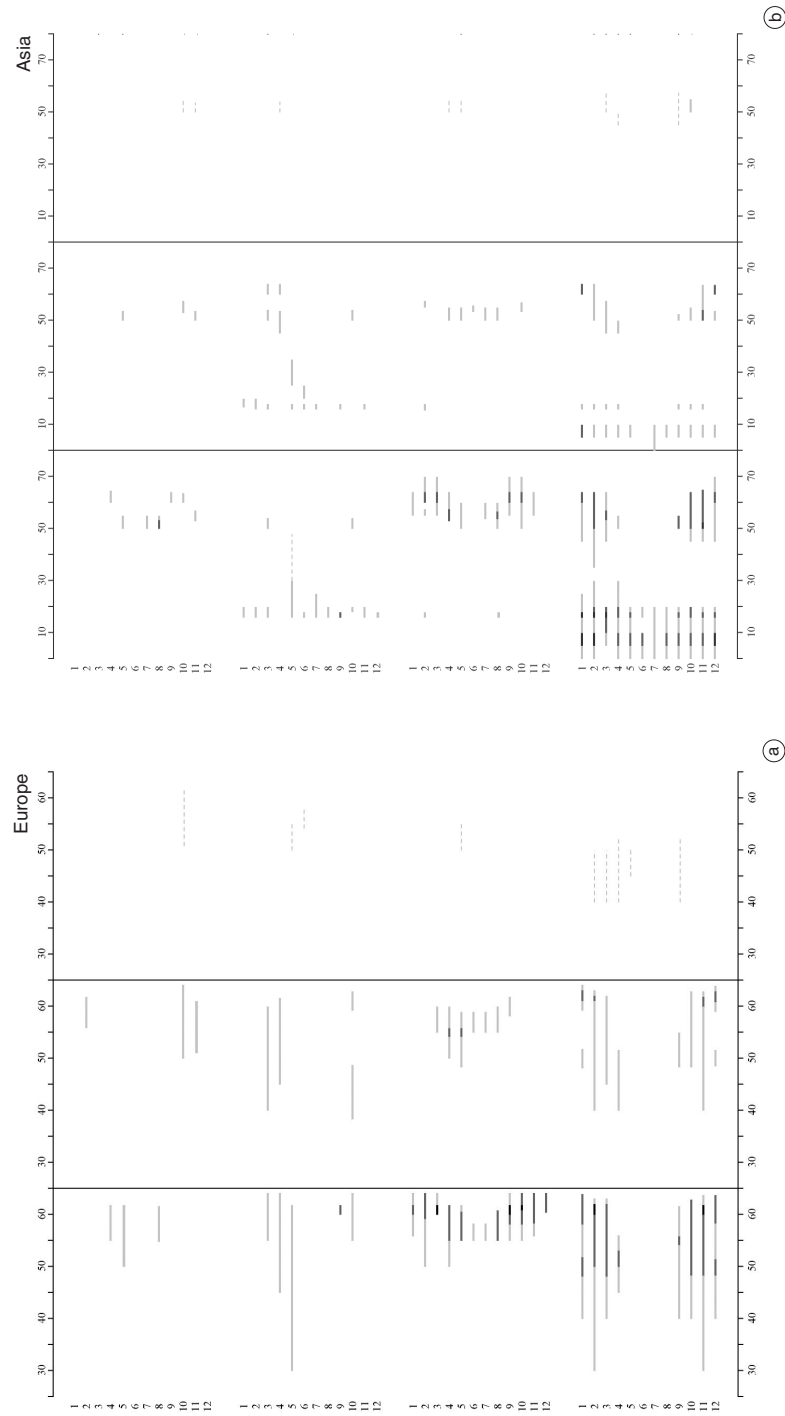


Fig. 4a,b. Frequency of occurrence of *negative* storms per month according to LT of commencement (from top to bottom: sunrise, day, sunset, night) and duration class (from left to right: small, medium, large duration) as a function of geomagnetic latitude (x-axis) in (a) Europe and (b) Asia (light grey: 0.5-1 storms/month, grey: 1-2 storms/month, dark grey: 2-3 storms/month, black: >3 storms/month).

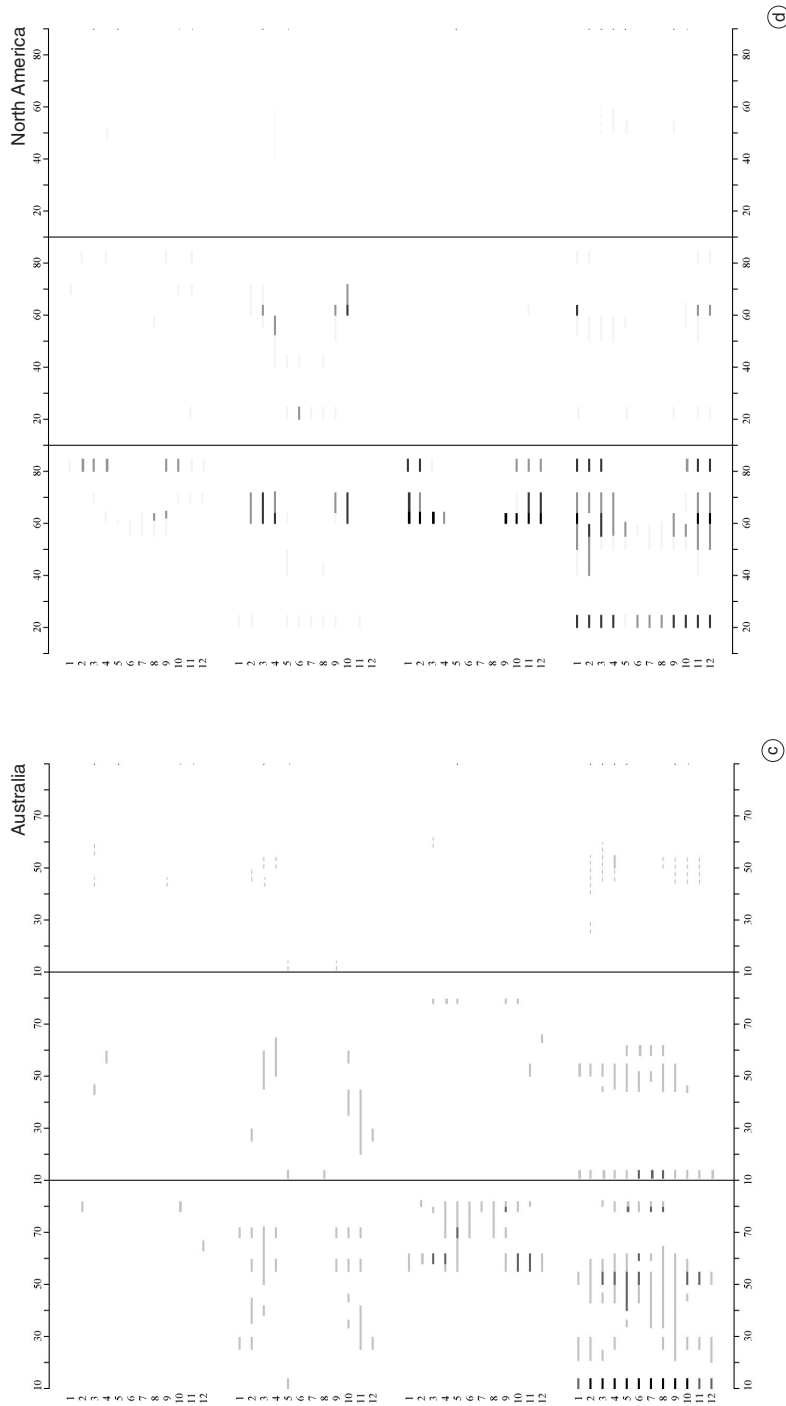


Fig. 4c,d. Frequency of occurrence of *negative* storms per month according to LT of commencement (from top to bottom: sunrise, day, sunset, night) and duration class (from left to right: small, medium, large duration) as a function of geomagnetic latitude (x -axis) in (c) Australia and (d) North America (light grey: 0.5-1 storms/month, dark grey: 2-3 storms/month and black: >3 storms/month).

for the Australian zone, where positive storms commencing in daytime are observed in summer at much higher latitudes (up to $75^\circ \varphi_m$). Furthermore the American zone is affected with greater frequency around $40^\circ \varphi_m$ by such phenomena, while the Asian sector is practically not at all affected above $30\text{--}40^\circ \varphi_m$. Positive storms of greater duration are frequent around $20^\circ \varphi_m$ and also about $60^\circ \varphi_m$ everywhere but in Asia.

Negative short duration disturbances are important all year long at the equatorial crest and mostly at about $60^\circ \varphi_m$ in the American zone during equinoctial months. However they are absent at low midlatitudes, except when phenomena of medium duration in American summer are concerned.

Sunset – Positive disturbances of short duration occur more frequently around $60^\circ \varphi_m$ all year, but summer, and they ‘penetrate’ to midlatitudes during winter, similarly to traveling ionospheric disturbances’ climatology (Hocke and Schlegel, 1996). This penetration to midlatitudes is *not* observed in the American and Australian sectors, presenting a UT effect. Furthermore, positive disturbances of greater duration (more than 5 h) affect mainly Europe.

On the contrary, negative storms occurring mostly during winter are observed from $60^\circ \varphi_m$ polewards, However, they affect European and Australian latitudes of about $55^\circ \varphi_m$ in summer. This is not the case in American sector. Again, longer duration negative storms occur only in Europe.

Night – Equatorial and lower midlatitudes present short- and medium-duration positive storms throughout the year, while at equinoxes and winter they also occur in mid- and highlatitudes. The only regions which present short-period positive storm effects in summer midlatitudes are the sectors including the geomagnetic poles (America and Australia). Longer duration positive effects are restricted to winter months in America and Asia, whereas Europe and Australia are also affected by such phenomena during equinoxes.

Negative storms present a similar frequency distribution in time and space with the formerly analysed positive ones.

Summarizing, the above results seem to confirm prominent features of ionospheric storms such as their local time and seasonal variation (Prölss, 1995; Mikhailov, 2000). However, here many regional and local phenomena are pointed out and users are provided with analytical maps of storm frequency.

4. Conclusions

The analysis of basic morphological storm features shows that positive storms present maximum power, *i.e.* depth and duration, in the equatorial anomaly crest and the auroral oval boundary, presenting durations of the order of 15 and 14 h, respectively. On the contrary, negative storms last longer at higher midlatitudes (around $50^\circ \varphi_m$), but their depth distribution with latitude is rather uniform.

The investigation of climatology has shown a different seasonal and spatial distribution of positive and negative storms according to their local time of commencement. Several regional phenomena have been identified, thus confirming that ionospheric storms can be regional. The morphology of these phenomena of local impact has to be examined in future investigations.

Acknowledgements

This work was supported by the Greek-Italian cultural collaboration (7th protocol).

REFERENCES

- ARAUJO-PRADERE, E.A., T.J. FULLER-ROWELL and M.V. CODRESCU (2002): STORM: an empirical storm-time ionospheric correction model, 1. Model description, *Radio Sci.*, **37** (5), 1070, doi: 10.1029/2001RS002467.
- ARAUJO-PRADERE, E.A., T.J. FULLER-ROWELL and D. BILITZA (2003): Validation of the STORM response in IRI 2000, *J. Geophys. Res.*, **108** (A3), 1120.
- BUONSANTO, M.J. (1999): Ionospheric Storms - A review, *Space Sci. Rev.*, **88**, 563-601.
- CANDER, L.R. (1993): On the global and regional behaviour of the mid-latitude ionosphere, *J. Atmos. Terr. Phys.*, **55**, 1543-1551.
- CANDER, L.R. and S.J. MIHAJLOVIC (1998): Forecasting ionospheric structure during the great geomagnetic storms, *J. Geophys. Res.*, **103**, 391-398.

- DANILOV, A.D. and L.D. MOROZOVA (1985): Ionospheric storms in the *F*2 region. Morphology and physics (review), *Geomagn. Aeron.*, **25**, 593-605.
- FOTIADIS, D.N., G.M. BAZIAKOS and S.S. KOURIS (2004): On the global behaviour of day-to-day MUF variation, *Adv. Space Res.*, **33** (6), 893-901.
- FULLER-ROWELL, T.J., M.V. CODRESCU, R.J. MOFFETT and S. QUEGAN (1994): Response of the thermosphere to geomagnetic storms, *J. Geophys. Res.*, **99** (A3), 3893-3914.
- FULLER-ROWELL, T.J., M.C. CODRESCU and P. WILKINSON (2000): Quantitative modeling of the ionospheric response to geomagnetic activity, *Ann. Geophysicae*, **18** (7), 766-781.
- GULYAeva, T.L. (1996): The 1996 Solar-Terrestrial Prediction Workshop, *IRI-News*, **3** (2), 6-7.
- HAIKOWICZ, L.A. (1998): Longitudinal (UT) effect in the onset of auroral disturbances over two solar cycles as deduced from the AE-index, *Ann. Geophys.*, **16**, 1573-1579.
- HOCKE, K. and K. SCHLEGEL (1996): A review of atmospheric gravity waves and travelling ionospheric disturbances: 1982-1995, *Ann. Geophysicae*, **14**, 917-940.
- JONES, K.L. (1971): Storm time variation of *F*2-layer electron concentration, *J. Atmos. Terr. Phys.*, **33**, 379-389.
- KOURIS, S.S., D.N. FOTIADIS and T.D. XENOS (1998): On the day-to-day variation of f_oF_2 and $M(3000)F_2$, *Adv. Space Res.*, **22** (6), 873-876.
- KOURIS, S.S., D.N. FOTIADIS and B. ZOLESI (1999): Specifications of the *F*-region variations for quiet and disturbed conditions, *Phys. Chem. Earth-Part C*, **24** (4), 321-327.
- MIKHAILOV, A.V. (2000): Ionospheric *F*2-layer storms, in *Fisica de la Tierra*, edited by M. HERRAIZ and B.A. DE LA MORENA, **12**, 223-262.
- PRÖLSS, G.W. (1993): On explaining the local time variation of ionospheric storm effects, *Ann. Geophysicae*, **11**, 1-9.
- PRÖLSS, G.W. (1995): Ionospheric *F*-region storms, in *Handbook of Atmospheric Electrodynamics* (Ed. Volland, CRC Press/Boca Raton), **2**, 195-248.
- PRÖLSS, G.W. and U. VON ZAHN (1978): On the local time variation of atmospheric-ionospheric disturbances, *Space Res.*, **18**, 159-162.
- RAWER, K. (1963): Propagation of Decameter waves (HF-band), in: *Meteorological and Astronomical Influences on Radio Wave Propagation*, edited by B. LANDMARK (Academic Press, New York), 221-250.
- SCHUNK, R.W. (Editor) (1996): *Handbook of Ionospheric Models, Special Report* (Boulder, U.S.A., Solar-Terrestrial Energy Program. STEP, Scientific Committee on Solar Terrestrial Physics, SCOSTEP).
- SZUSZCZEWICZ, E.P., M. LESTER, P. WILKINSON, P. BLANCHARD, M. ABDU, R. HANBABA, K. IGARASHI, S. PULINETS and B.M. REDDY (1998): A comparative study of global ionospheric responses to intense magnetic storm conditions, *J. Geophys. Res.*, **103** (A6), 11665-11684.
- WILKINSON, P.J. (1995): Predictability of ionospheric variations for quiet and disturbed conditions, *J. Atmos. Solar-Terr. Phys.*, **57** (12), 1469-1481.
- YEH, K.C., S.Y. MA, K.H. LIN and R.O. CONKRIGHT (1994): Global ionospheric effects of the October 1989 geomagnetic storm, *J. Geophys. Res.*, **99** (A4), 6201-6218.

(received January 23, 2004;
accepted June 17, 2004)